# OH FLUORESCENCE IMAGES OF PULSED FLAME JET IN A SWIRL FLOW

**E. MURASE, K. HANADA, T. HAMAKAWA, and K. HOTTA**
KYUSHU UNIVERSITY

6-10-1 Hakozaki, Higashi-ku, Fukuoka 812-8581, Japan
E-mail: murase@mech.kyushu-u.ac.jp

*Key words*: Internal Combustion Engine, Ignition, OH Radical, Planar Laser-Induced Fluorescence, Pulsed Flame Jet, Spark Discharge

## INTRODUCTION

In internal combustion engines, lean-burn is particularly attractive for minimizing pollutant emissions, in particular NOx, with a concomitant improvement in fuel economy. For combustion in lean fuel-air mixtures, achievement of adequate reliability of ignition and sufficiently high burning rate requires special devices. The most effective among them is the injection of active radicals by means of Pulsed Flame Jet (PFJ) ignition system (Oppenheim *et al.*, 1990; Hensinger *et al.*, 1993; Murase *et al.*, 1994, 1996; Murase and Hanada, 2001, Wolanski *et al.*, 1997). Presented here is an experimental proof of the action of OH radical produced by such an ignition system in a swirl flow with varying the spark discharge mode in the cavity of the PFJ igniter. The measuring apparatus used for this purpose was based on the Planar Laser-Induced Fluorescence (PLIF) method, and the effects of spark discharge mode in the cavity of the PFJ igniter on the variation of OH fluorescence area in the jet and its intensity were revealed quantitatively.

## EXPERIMENTAL APPARATUS

**PFJ IGNITER** The PFJ igniter (Murase *et al.*, 1994, 1996; Murase and Hanada, 2001) is of the same size and shape as the conventional spark plug, and it contains a small cavity and an orifice as depicted in Fig. 1. Rich fuel-air mixture was injected by the fuel injector and it was introduced into the cavity via a check valve, an insulator, a hollow electrode, and two inlet ports. Then it was ignited by the spark discharge between the hollow electrode and the orifice plate. Thus a jet of incomplete combustion products was issued from the orifice to form a turbulent jet plume where the process of combustion in the combustion chamber was initiated. The cavity dimensions and the operating conditions of the PFJ igniter are presented in Table 1. The fuel used was a methane-air mixture, and the equivalence ratio in the combustion chamber was 0.8 and that in the cavity was 1.5.

**COMBUSTION CHAMBER AND LIF SYSTEM** The combustion chamber used in OH fluorescence measurements is shown in Fig. 2. It was made out of two cylinders of 60 mm in diameter, joined together in the middle. Quartz glass windows were equipped at four opposite ends, and the PFJ igniter was installed at the top of the chamber. The inlet port for the mixture was located at the bottom, which was connected with a mixture storage vessel via a solenoid valve. The inlet port was directed tangential to an imaginary circle with diameter of 39 mm, which created a large rotating motion of the mixture, namely, a swirl in the chamber. In the combustion tests, the opening and closing timing of the solenoid was controlled so that the swirl speed and the pressure in the chamber at the time of ignition was 10 m/s and at atmospheric pressure respectively.

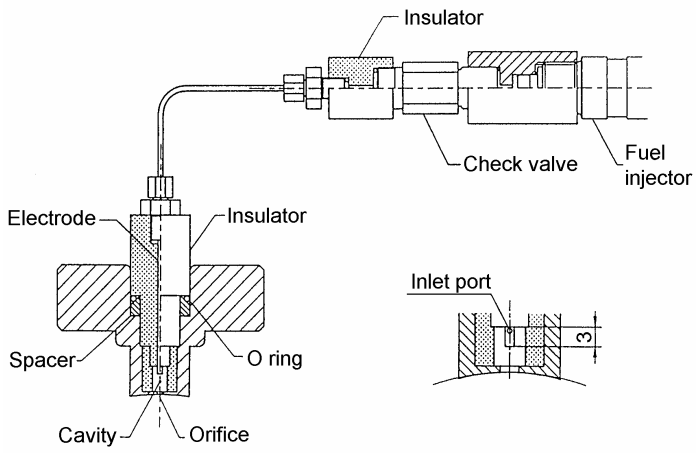


Fig. 1 PFJ ignition system

Table 1 Cavity dimensions and operating conditions of PFJ igniter

| | |
|---|---|
| Cavity volume / mm$^3$ | 170 |
| Orifice diameter / mm | 2.5 |
| Gated width of injector trigger / ms | 55 |
| Ignition delay* / ms | 50 |

* time interval between triggers for injector opening and start of ignition spark discharge

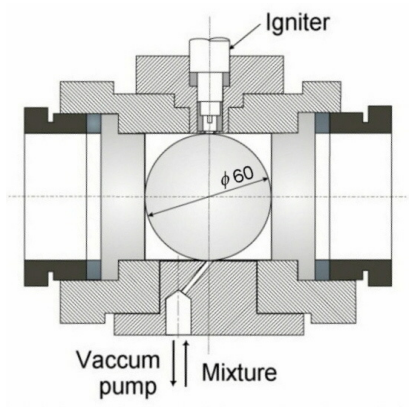


Fig. 2 Combustion chamber

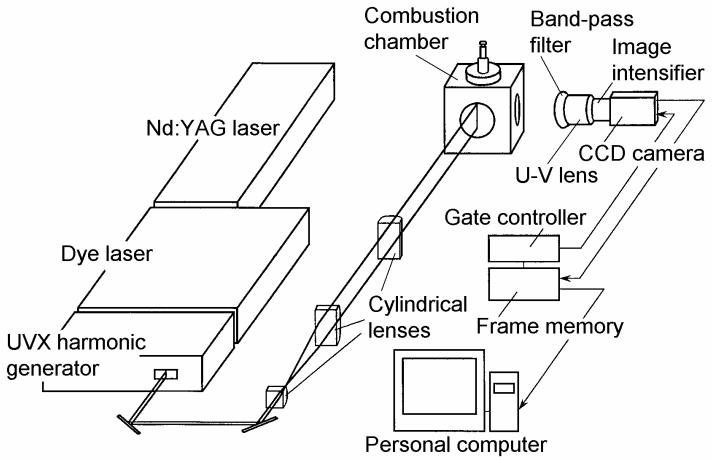


Fig. 3 Schematic diagram of experimental setup for OH fluorescence measurements

The experimental setup for PLIF is shown schematically in Fig. 3. In OH fluorescence measurements, OH was pumped at the X $^2\Pi$ (ν = 1) – A $^2\Sigma$(ν = 0) transition at 283 nm, and the fluorescence from the A $^2\Sigma$(ν = 0) – X $^2\Pi$ (ν = 0) transition was collected (Hanson, 1986; Murase and Hanada, 2001). The height and the thickness of the laser sheet were about 60 mm and 0.5 mm respectively. The fluorescence from the excited OH was collected with a UV lens and a band-pass filter (Central wavelength: 307.8 nm, Half width: 14.1 nm, Maximum transmissivity: 20.5 %), and imaged by a time-gated ICCD camera. In order to eliminate OH emission at 306.4 nm, the gate width of the ICCD camera used was 100 ns. It is of importance to note that the OH fluorescence images provided in this paper are nonconsecutive, i.e., each image was acquired from a different combustion test.

## RESULTS AND DISCUSSIONS

**OH EMISSION IN PFJ** In order to clarify the effect of spark discharge characteristics in the cavity on the production of OH radical in PFJ, four different spark discharge modes were investigated. Figure 4 depicts the schematic diagrams of the spark discharge voltage of each mode as a function of time. The normal (Fig. 4-a1) was the spark discharge mode using in the ordinary ignition system of the commercial cars. The double (Fig. 4-a2) and the triple (Fig. 4-a3) modes were realized using the same ignition circuit as used in the normal mode but different ignition trigger pulse modes. That is, two ignition trigger pulses at an interval of 2 ms were provided in the double mode, and three ignition trigger pulses were provided in the triple mode as depicted in Fig. 4. On the other hand, the long mode (Fig. 4-b) was realized using the different ignition coil which had a large inductance. In all spark discharge modes, the gated width of the injector trigger and the ignition delay were fixed at 55 and 50 ms respectively, as shown in Table 1. Here, the ignition delay in double and triple modes was defined as the time interval between triggers for injector opening and the start of the first spark discharge.

Figure 5 shows typical examples of OH fluorescence images. The diameter of the region viewed was 60 mm, and the degree of brightness of the images corresponds to the OH fluorescence intensity. As the fresh mixture in the chamber was entrained into the jet from the side of the jet by the swirl, the jet issuing from the orifice was deflected towards the chamber wall as shown in Fig. 5. Therefore, the incomplete combustion

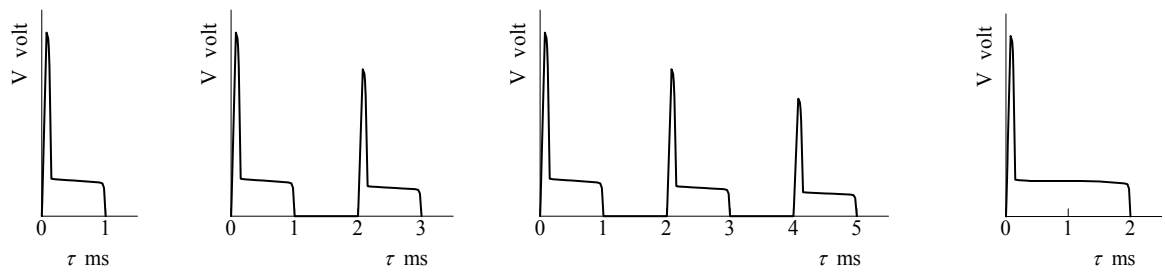


(a1) Normal (a2) Double (a3) Triple (b) Long

Fig. 4 Schematic diagrams of spark discharge voltage in PFJ igniter

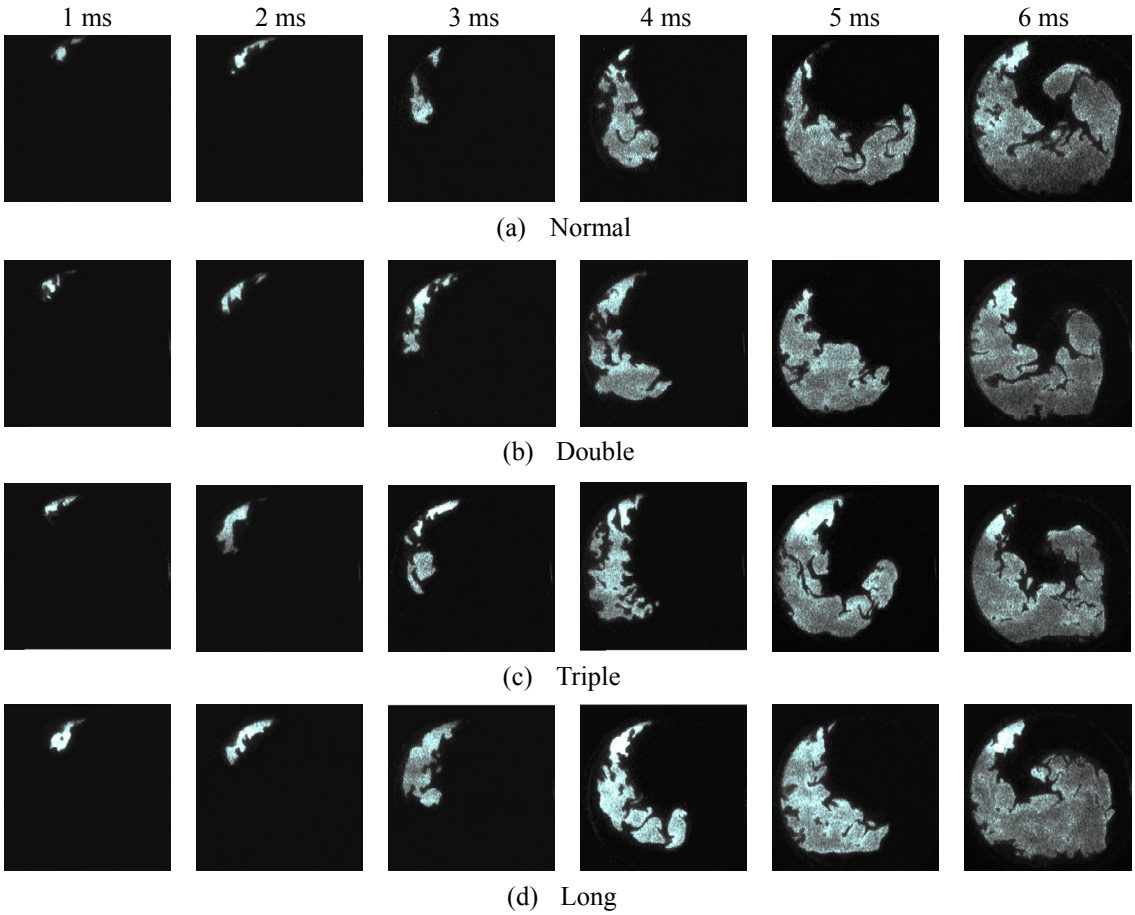


Fig. 5 PLIF images of OH after start of spark discharge

products just issued from the orifice entrained the fresh mixture continuously during its injection period. As a result, the very intense OH fluorescence was observed near the orifice corresponding to the spark discharge characteristics in the cavity. In ordinary laminar flames, the intense OH fluorescence can be seen at the periphery of the flames (Murase *et al.*, 1994), however, the intense OH fluorescence in Fig. 5 can be seen inside the jet, which is the evidence of the volumetric combustion in PFJ (Murase *et al.*, 1994). Considering that the black region must corresponds to the unburned region, most of the images after 3 ms have deeply indented unburned regions in the jet. Furthermore, separated OH fluorescence regions could be seen in some cases.

In order to understand the characteristics of OH fluorescence quantitatively, the variation of OH fluorescence area, its mean intensity, and the total intensity with delay time after the start of the first spark discharge, $\tau$, are depicted in Figs. 6, 7, and 8 respectively. Here, the mean intensity and the total intensity were defined by the intensity averaged by its fluorescence area and the intensity integrated over the whole fluorescence area, respectively. According to Fig. 6, the OH fluorescence area increased monotonously with time, $\tau$, and until 6 ms, a certain difference in the OH fluorescence area was existed. As compared with the normal mode, the other three modes showed larger OH fluorescence area, and the long mode had the largest OH fluorescence area until 4 ms. After 4 ms, the triple mode showed the largest OH fluorescence area. As shown in Fig. 4, the triple mode had its third spark discharge between 4 and 5 ms, which must be the reason of increasing the OH fluorescence area by the triple mode after 4 ms. Similar to this reason, as the second spark discharge in the double and the triple modes occurred between 2 and 3 ms, larger OH fluorescence areas were created by the double and the triple modes after 2 ms. According to Fig. 7, the variation of the mean OH fluorescence intensity obtained by the long mode was different from those obtained by the normal, double, and triple modes. The long mode had higher mean OH fluorescence intensity from the beginning, which must be caused by the difference in the ignition coil used. From this point of view, the use of the large inductance coil has a better performance in creating OH radicals in the jet. In the normal, double, and triple modes, the first peak of the mean OH fluorescence intensity was observed at 3 ms, and another peak was observed at 5 ms in the triple mode. The reason why the first peak of the mean OH fluorescence intensity was observed at 3 ms in spite of different spark discharge mode is not certain, however, the second spark discharge in the double and triple modes increased the mean OH fluorescence intensity in the jet. The occurrence of the second peak of the OH fluorescence intensity in the triple mode corresponded with the time of the third spark discharge. All the

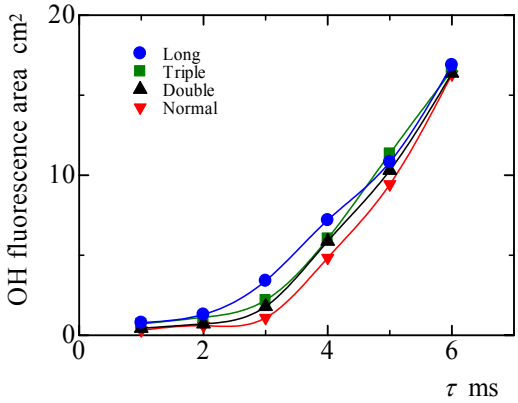


Fig. 6 Variation of OH fluorescence area with delay time after start of spark discharge

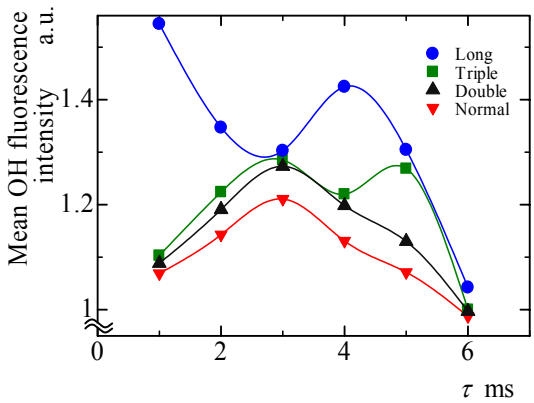


Fig. 7 Variation of mean OH fluorescence intensity with delay time after start of spark discharge

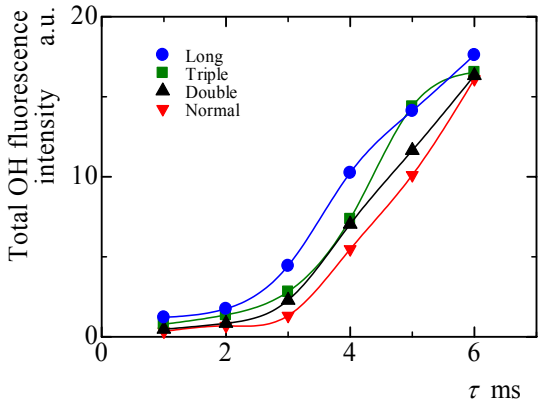


Fig. 8 Variation of total OH fluorescence intensity with delay time after start of spark discharge

mean OH fluorescence intensity approached to the same value at 6 ms, where the influences of the active jet issuing from the orifice must be diminished. As it appears from Fig. 8, the effects of the spark discharge mode on the total OH fluorescence intensity were similar to those on the OH fluorescence area shown in Fig. 6. Therefore, the total fluorescence intensity was mostly governed by the OH fluorescence area.

## CONCLUSIONS

(1) In the swirl flow, the very intense OH fluorescence was observed near the orifice, and images of deeply indented unburned regions and separated OH fluorescence regions could be seen in PFJ.

(2) The spark discharge mode in the cavity of the PFJ igniter affected the variation of OH fluorescence area and its intensity in the jet, and the use of the large inductance coil had a better performance in creating OH radicals in the jet.

## REFERENCES


Hanson, R.K. (1986). Combustion Diagnostics: Planar Imaging Techniques. *Twenty-first Symposium (International) on Combustion*, pp. 1677-1691, The Combustion Institute.

Hensinger, D.M., Maxson, J.A., Hom, K., and Oppenheim, A.K. (1993). Jet Plume Injection and Combustion. *SAE Trans.*, **101**, Sec.3, pp. 571-580.

Murase, E., Ono, S., Hanada, K., and Oppenheim, A.K., (1994). Pulsed Combustion Jet Ignition in Lean Mixtures. *SAE Paper* No. 942048.

Murase, E., Ono, S., Hanada, K., and Oppenheim, A.K. (1996). Initiation of Combustion in Lean Mixtures by Flame Jets. *Combustion Science and Technology*, **113-114**, pp.167-177.

Murase, E. and Hanada, K. (2001). Enhancement of Combustion by Injection of Radicals. *SAE Trans*., **109**, Sec. 3, pp. 34-41.

Oppenheim, A.K., Beltramo, J., Faris, D.W., Maxson, J.A., Hom, K., and Stewart, H.E. (1990). Combustion by Pulsed Jet Plumes - Key to Controlled Combustion Engines. *SAE Trans.*, **98**, Sec. 3, pp. 175-182.

Wolanski, P., Dabkowski, A., and Przastek, J. (1997). Influence of PJC Ignition on Efficiency and Emission of IC Piston Engine Operating at Partial and Full. *SAE Paper* No. 972871.